3-D Reconstruction of Underwater Objects Using Arbitrary Acoustic Views

Seungchul Kwak[1], Yonghoon Ji[1], Atsushi Yamashita[1], and Hajime Asama[1]

Abstract— This paper presents a method for 3-D measurement of underwater objects using acoustic cameras. The 3-D measurement of underwater objects using arbitrary acoustic views is a major advantage to grasp underwater situations. Robots such as autonomous underwater vehicles (AUVs) and remotely operated underwater vehicles (ROVs) are desired to mount acoustic cameras for underwater investigations, especially in turbid or deep environments. Acoustic cameras are the most powerful sensors for acquisition of underwater information because they have no limitation in their visibility. Furthermore, their sensing area covers wide range, which is often the limitation of traditional sonar sensors. However, 3-D reconstruction systems using acoustic images from arbitrary acoustic views have not been established even with their undeniable worth. In this paper, we propose a novel approach which enables 3-D measurements of underwater objects using arbitrary viewpoints. This approach contributes to establishing a methodology for 3-D shape reconstruction systems, where the correspondences between feature points on each acoustic image are described. The experimental results indicate not only the validity of our proposed approach, but also that the novel methodology demonstrates superior performance in estimating 3-D information of underwater objects.

I. INTRODUCTION

There are numerous cases in which hazardous environment limits human access but accessibility is essential at times despite its potential danger. For such cases, rescue robots are widely implemented and perform various tasks to protect people and to prevent secondary disasters. For example, the underwater robotic systems were operated in the spent fuel pool of unit 4 of the Fukushima Daiichi nuclear power station, which has been confronting a crisis since a massive earthquake occurred in eastern Japan, to acquire information concerning with used fuel assemblies and debris in the pool [1]. For such rescue missions and other various underwater tasks, underwater target recognition plays a major role. Thus, operating underwater tasks requires accurate acquisition of underwater image information. There are some specific sensors that are suitable for acquisition of underwater information. Optical cameras were used in numerous researches to operate underwater simultaneous localization and mapping (SLAM) [2], underwater investigation [3], and 3-D reconstruction of underwater objects [4]. This is due to optical camera's ability to provide high resolution image with high accuracy. However, there is a limit to what the optical cameras can recognize, notably in turbid or deep water. A laser sensor system for underwater target recognition is also proposed [5]; however, such high-frequency signal attenuates fast underwater. To this end, sonar sensors are most commonly used for underwater tasks. However, traditional sonar sensors require improvements in resolution because of their limitation on detail characterizations of underwater imaging. One research utilized acoustic lens to improve resolution as it produces denser acoustic waves [6]. Another research proposed probabilistic approach to specify the range of acoustic waves using acoustic energy function, resulting in improved performance of acoustic imaging [7]. However, traditional sonar sensors cannot fully grasp underwater situation as they lack accuracy in underwater imaging. On the other hand, in recent years, 2-D imaging sonars which are called acoustic cameras such as BlueView [8], DIDSON (*D*ual-Frequency *ID*entification *SON*ar) [9], ARIS (Adaptive Resolution Imaging Sonar) [10] have gained popularity with their provision of high resolution acoustic images even in turbid water. Moreover, they cover wide range of fields and overcome difficulties in identification of underwater objects which are often the limitation of traditional sonar sensors [11]. However, acoustic images are very dissimilar to optical images as shown in Fig. 1, because acoustic cameras perform unique signal processings. These unique characteristics of acoustic cameras have been preventing the establishment of 3-D reconstruction model.

A previous research has proposed method to predict what
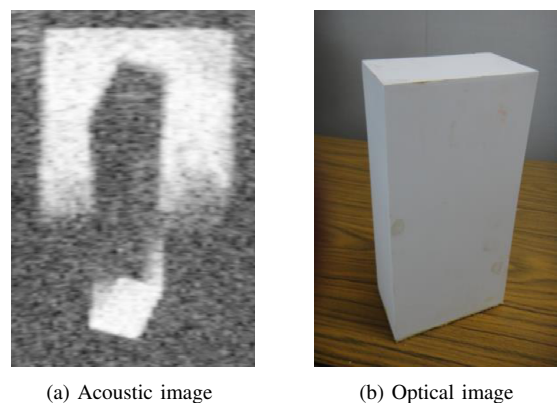
(a) Acoustic image   (b) Optical image

Fig. 1. Comparison of acoustic image and optical image. Although the subject is not only identical (cuboid) but also taken from almost same viewpoint, acoustic image is very dissimilar to optical image.

the underwater objects are by comparing similarities between real-time acoustic images and prepared database [12]. This approach could identify underwater objects only with pre-established database. In other words, it could not identify the objects if their information has not been pre-established. Another research has proposed method for system calibration and 3-D scene reconstruction by opti-acoustic stereo imaging [13]. Although this study improved accuracy for 3-D reconstruction of underwater objects by the opti-acoustic stereo imaging system calibration, it still relies on the optical vision. The limitation that the method is restricted to clear water remains unsolved problem. Another research utilized concentrator lens for acoustic camera to obtain 3-D information of underwater objects. The concentrator lens not only allows acoustic camera beams to propagate further, but also solves problem concerning omission of elevation angle (described in Section 2), which is the main difficulty of acoustic cameras for 3-D reconstruction [14]. However, this method fails 2-D imaging, a major benefit of acoustic cameras. The 3-D reconstruction system for underwater environments using multiple acoustic images from different views has been previously proposed [15]. This approach deals with the problem on determining the missing elevation information by proposing geometric model. However, this system limits the movement of acoustic cameras to a vertical motion. Consequently, the system cannot deal with determining the 3-D shape of underwater objects from arbitrary viewpoints.

Therefore, this paper improves and extends the previous work on using multiple acoustic images with different approach. We propose a novel geometric approach to measure 3-D coordinates of feature points on acoustic images from arbitrary acoustic views, by using pose relationships among each viewpoint. Such utilizations of pose relationships among each viewpoint allows 3-D shape reconstruction of underwater objects.

The contribution of this research is as follow. This research deals with the problem on the previous research. As described above, the 3-D reconstruction system using acoustic images from arbitrary viewpoints has not been established. Therefore, this research proposes theoritical methodology for 3-D reconstruction of underwater objects using arbitrary acoustic views. Moreover, this paper indicates that our research successfully dealt with 3-D reconstruction of underwater objects by implementing the proposed geometric approach.

The remainder of this paper is organized as follows. Section 2 provides preliminaries on the principles of the acoustic cameras. In Section 3, the proposed 3-D shape reconstruction model is presented. Section 4 deals with the results of the experiments. The discussions for the experimental results are described in Section 5. The final section concludes the paper and points out future prospects.

II. PRELIMINARIES

In this section, an acoustic projection model and an imaging geometry model are described to explain the principles of the acoustic cameras. These models are depicted clearly in [17]. Difficulties regarding 3-D reconstruction using acoustic images can be recognized by these models.

A. Acoustic Projection Model

The acoustic cameras insonify acoustic waves in forward direction to generate an acoustic image. The sensing area is determined by maximum range r_{cam}, azimuth angle θ_{cam}, and elevation angle ϕ_{cam} as shown in Fig. 2. These parameters depend on the specifications of the acoustic cameras. Acoustic waves propagate within the scope of the determined sensing area. When traveling forward, the acoustic waves hit underwater objects. This results in reflections of the acoustic waves in different directions from an original direction of propagation. The sound energy of acoustic waves diminishes with distance and reflection. The reflected acoustic waves are processed by an array of transducers as a function of the measurement range r, the azimuth angle θ, and the diminished sound energy W.

B. Imaging Geometry Model

A pixel coordinate system of an acoustic image is determined by the measurement range r and the azimuth angle θ through the processing of an array of transducers. The major problem with this phenomenon is that the elevation angle ϕ cannot be acquired from an acoustic image. Accordingly, the image plane is proposed to describe displaying mechanism of the acoustic cameras [16]. Targets detected by the acoustic waves are projected on the image plane along the arc defined by the elevation angle. In this way, the data overlap at the same point when multiple acoustic waves travel the same distance. When the data overlap, the aggregate of each point's sound energy is mapped on the acoustic image [17]. These phenomena make it difficult to analyze the acoustic images [18].

III. METHODOLOGY

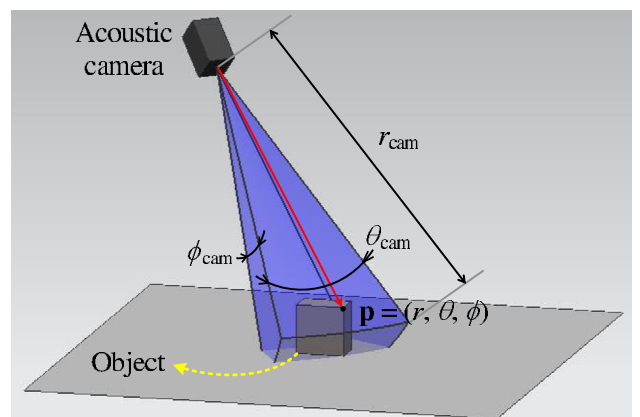As mentioned in Section 2, an acoustic image is described by three parameters: the measurement range r, the azimuth

Fig. 2. Acoustic projection model. The sensing area is determined by maximum range r_{cam}, azimuth angle θ_{cam}, and elevation angle ϕ_{cam}. The feature point $\mathbf{p}$ is detected as acoustic camera coordinates (r, θ, ϕ).

angle θ, and the diminished sound energy W. Therefore, it is impossible to recover 3-D information of objects from an acoustic image, because elevation angle ϕ is missing. However, elevation angle ϕ can be determined by using two different acoustic visions whose pose relationship is known. In this section, a theoritical methodology for 3-D reconstruction is presented to measure 3-D coordinates of underwater objects. The proposed model deals with the pixel coordinate system of acoustic images, which makes it free from the problem of scattering or noise in the acoustic images.

A. Feature Points on Acoustic Image

An extraction of feature points on an acoustic image is an important task because it is necessary to identify the correspondence between two acoustic images. Feature points indicate distinguishable points on acoustic images. For instance, vertex or area whose material is different from each other can be considered as feature points because sound energy changes rapidly with such structures.

B. Candidates for Feature Point

While it is impossible to acquire exact 3-D coordinates of feature point $\mathbf{p}$ in Fig. 2, the values for the measurement range r and the azimuth angle θ are obtainable from pixel coordinates of the acoustic image. Regarding the value of elevation angle ϕ, it is described by candidates which are presumably the real coordinate of the feature point $\mathbf{p}$. The candidates are established based on the specifications of the acoustic camera. Accordingly, the feature point $\mathbf{p}$ which is projected from viewpoint 1 can be represented as

$$^{v_1}\mathbf{p}_i = [^{v_1}r, {}^{v_1}\theta, {}^{v_1}\phi_i]^{\mathrm{T}}, \tag{1}$$

where i indicates the index of candidates, assuming

$$0 \leq {}^{v_1}\phi_i \leq \phi_{\text{cam}}. \tag{2}$$

Set of candidates for feature point $\mathbf{p}$ from viewpoint 1 is

$$^{v_1}\mathbf{P} = [^{v_1}\mathbf{p}_1 \cdots {}^{v_1}\mathbf{p}_i \cdots {}^{v_1}\mathbf{p}_I]^{\mathrm{T}}, \tag{3}$$

where I indicates the number of candidates concerned with the viewpoint 1. The larger the number of candidates, the accuracy improves because the candidate points are denser.

Similarly, the feature point $\mathbf{p}$ which is projected from viewpoint 2 can be represented as

$$^{v_2}\mathbf{p}_j = [^{v_2}r, {}^{v_2}\theta, {}^{v_2}\phi_j]^{\mathrm{T}}, \tag{4}$$

where j indicates the index of candidates, assuming

$$0 \leq {}^{v_2}\phi_j \leq \phi_{\text{cam}}. \tag{5}$$

Set of candidates for feature point $\mathbf{p}$ from viewpoint 2 is

$$^{v_2}\mathbf{P} = [^{v_2}\mathbf{p}_1 \cdots {}^{v_2}\mathbf{p}_j \cdots {}^{v_2}\mathbf{p}_J]^{\mathrm{T}}, \tag{6}$$

where J indicates the number of candidates concerned with the viewpoint 2.

C. 3-D Reconstruction of Feature Points

3-D coordinates of the feature point cannot be obtained by using single acoustic image. However, two different acoustic visions whose poses are known allow us to determine 3-D coordinates. It is because two arcs made of candidate points concerning with each viewpoint intersect at one point as shown in Fig. 3.

In our proposed model, set of candidates from each viewpoint with minimum distance are adopted for the determination of the 3-D reconstruction of feature points. The 3-D feature points are defined by mean value of the adopted candidates. Defining the feature point's 3-D coordinates by using mean value copes with the problem when two arcs do not intersect at one point during implementation. Moreover, as the mean value is supposed to be the real value, defining the feature point's 3-D coordinates by using mean value contributes to obtaining correct 3-D information. In that process, candidates which are described in local spherical coordinate system are needed to be represented in global Cartesian coordinate system.

By using the relationship between spherical and Cartesian coordinates, and homogeneous transformation matrix, candidates for the feature point $\mathbf{p}$ of viewpoint 1 which are described in local spherical coordinate system can be represented in global Cartesian coordinate system as follow:

$$^{v_1}\mathbf{p}_i^{\text{Car}} = [x_i, y_i, z_i]^{\mathrm{T}}. \tag{7}$$

Similarly, candidates for the feature point $\mathbf{p}$ of viewpoint 2 which are described in local spherical coordinate system can be represented in global Cartesian coordinate system as follow:

$$^{v_2}\mathbf{p}_j^{\text{Car}} = [x_j, y_j, z_j]^{\mathrm{T}}. \tag{8}$$

Therefore, the distance $l(i, j)$ between candidates from each viewpoint is

$$l(i, j) = \sqrt{(x_i - x_j)^2 + (y_i - y_j)^2 + (z_i - z_j)^2}. \tag{9}$$

When it is supposed that $(i_{\min}, j_{\min})$ are indices which make distance (9) smallest, the indices are obtained by

$$(i_{\min}, j_{\min}) = \underset{1 \leq i \leq I, 1 \leq j \leq J}{\arg\min} \, l(i, j). \tag{10}$$

Hence, by averaging candidates on index $i_{\min}$ and $j_{\min}$, 3-D coordinates of the feature point $\hat{\mathbf{p}}^{\text{Car}}$ are derived as follow:

$$\hat{\mathbf{p}}^{\text{Car}} = \begin{pmatrix} \dfrac{x_{i_{\min}} + x_{j_{\min}}}{2} \\ \dfrac{y_{i_{\min}} + y_{j_{\min}}}{2} \\ \dfrac{z_{i_{\min}} + z_{j_{\min}}}{2} \end{pmatrix}. \tag{11}$$

Note that calculating an intersection of interpolated arcs directly can also be considered; however, the intersection point may not exist due to various noises. Therefore, we apply the approach that search a minimum value of distance.
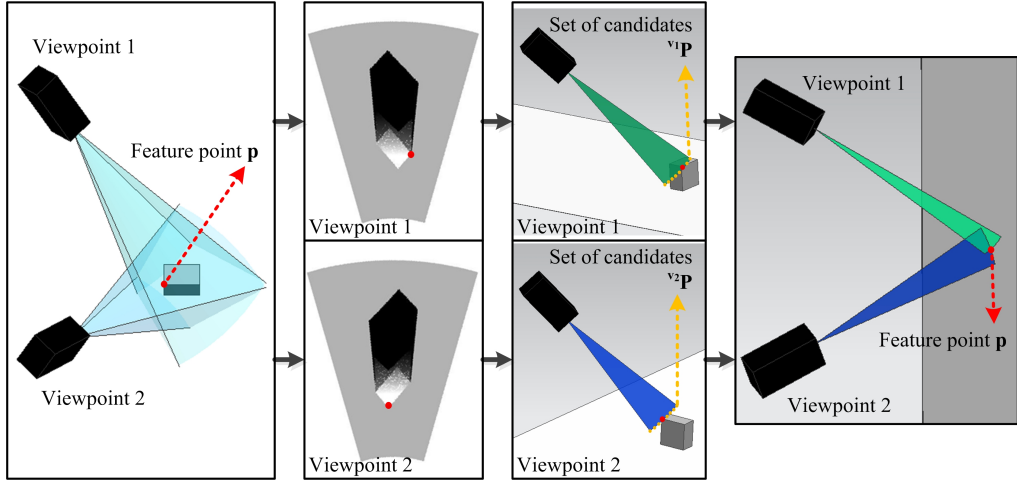
Fig. 3. Determination of feature point's 3-D coordinates. After feature point **p** on acoustic image is extracted, set of candidates ^{v_1}P and ^{v_2}P for the feature point are described as form of arc. As the pose relationship between two acoustic views is known, two arcs associated with each acoustic views intersect at one point. As a result, 3-D coordinates of the feature point **p** is analytically derived.

The 3-D coordinates of the feature point **p** are analytically derived by the processes mentioned above. By extracting multiple feature points on acoustic image, it is possible to reconstruct 3-D shape of underwater objects.

IV. EXPERIMENTAL RESULTS

In this section, simulation results are described to verify the validity of our proposed methodology. By using the model represented in Section 3, we preferentially conducted experiments for obtaining 3-D information of artificial underwater objects. A simulator developed by our group was used for the experiments [17]. We used a cuboid and a triangular prism for the underwater object as their multiple vertices allow us to extract highly distinguishable feature points from acoustic images.

A. Feature Points on Acoustic Image

The acoustic images of the cuboid and the triangular prism are shown in Figs. 4 and 5 respectively. Figures 4(a) and 5(a) are acoustic images associated with viewpoint 1, and Figs. 4(b) and 5(b) are acoustic images associated with viewpoint 2. Points marked on each acoustic image are manually designated not only to indicate the feature points but also to demonstrate the correspondence between two acoustic images. It is possible to identify the shape of objects by recovering the 3-D coordinates of each designated feature point.

In these simulation experiments, we utilized the specifications of ARIS EXPLORER 3000 for the acoustic cameras [19]. The specifications are shown in Table I.

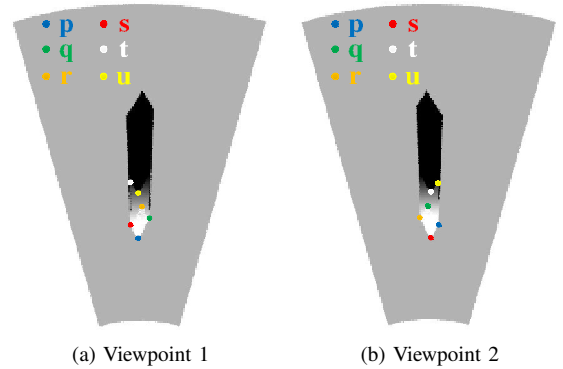(a) Viewpoint 1   (b) Viewpoint 2

Fig. 4. Acoustic images of cuboid associated with each acoustic view. Points marked on each acoustic images indicate the feature points to estimate 3-D coordinates. Additionally, the marks demonstrate the correspondence between two acoustic images.
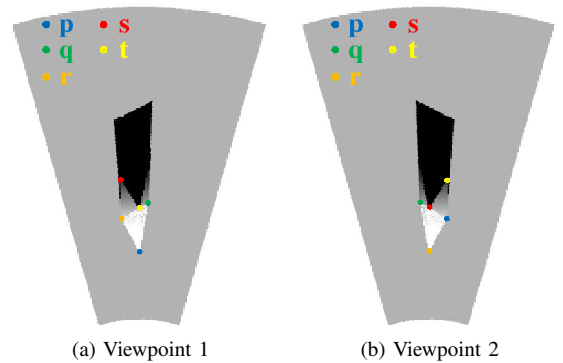

(a) Viewpoint 1   (b) Viewpoint 2

Fig. 5. Acoustic images of triangular prism associated with each acoustic view. Points marked on each acoustic images indicate the feature points to estimate 3-D coordinates. Additionally, the marks demonstrate the correspondence between two acoustic images.

B. Candidates for Feature Point

Identifying the pixel coordinates of the feature points from acoustic images allows us to obtain the measurement range and the azimuth angle (r, θ) with regard to each feature point.

TABLE I
SPECIFICATIONS OF ARIS EXPLORER 3000

Identification range r_{cam}	5 m
Azimuth angle θ_{cam}	32 deg
Elevation angle ϕ_{cam}	14 deg
Number of transducer beams	128
Beam width	0.25 deg

Candidates for each feature point with respect to viewpoint 1 are described in the form of Eq. (1), where $i = 0, 1, \cdots, 1400$, and $^{v1}\phi_i = \phi_{cam} - 0.01i$ [deg].

In the same way, candidates for each feature point with respect to viewpoint 2 are described as the form of Eq. (4), where $j = 0, 1, \cdots, 1400$, and $^{v2}\phi_j = \phi_{cam} - 0.01j$ [deg].

C. Determination of Feature Point's 3-D Coordinates

By the processes described in Section 3, the 3-D measurement of each feature point is performed. Figure 6, Tables II and III show the simulation results relating to the cuboid, and Fig. 7, Tables IV and V show those relating to the triangular prism. As described in Figs. 6 and 7, the 3-D coordinates of vertices from the cuboid and the triangular prism are estimated. The red circle marks indicate the ground truth coordinate values, and the blue diamond marks indicate the estimated coordinate values. Tables II, III, IV, and V show the results of the estimated value with respect to the ground truth and root mean square errors respectively.

V. DISCUSSION

As shown in Tables III and V, approximately 0.002~0.009 m error occurred. Two possible reasons can be considered about the occurrence of the errors.

The first reason is the accuracy problem on pixel coordinates of acoustic images. While the coordinates in the real space are successive, those in the acoustic image are discrete. The signal processing and displaying mechanisms of acoustic cameras can only represent the real number coordinates as integers.

The second reason is the problem on a beam width. As shown in Table I, ARIS EXPLORER 3000 has 128 transducer beams. The insonified acoustic waves are processed by 128 transducers, which means that the azimuth angle θ_{cam} is divided into 128 beam slices (Fig. 8(a)). As a result, the beam width of each beam slice is 0.25 deg as shown in Fig. 8(b). Therefore, errors resulting from the beam width is hardly avoidable. In this simulation experiments, the underwater objects were located at approximately 2 m from the acoustic camera, resulting in occurrence of the approximately 0.009 m error (Fig. 8(b)).

For these reasons, the errors shown in Tables III and V occurred, however, as the errors were below 0.009 m, the validity of our proposed method was verified.

However, unless there are distinguishable feature points on acoustic images, the 3-D shapes of underwater objects are hardly identifiable. For instance, hemisphere has no vertex, resulting in absence of feature points on acoustic images. Moreover, correspondences between two different acoustic views are difficult to describe as shown in Fig. 9. Thus, there still remains future works on such structures with no distinguishable feature points.
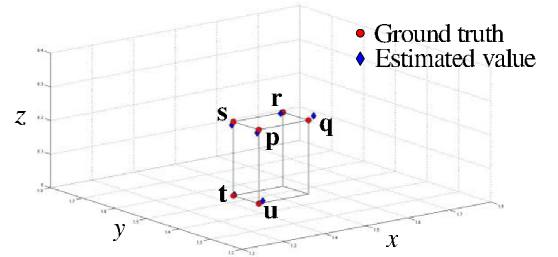

Fig. 6. Experimental results of cuboid. 3-D coordinates of cuboid's 6 vertices are estimated. The red circle marks indicate the ground truth, and the blue diamond marks indicate the estimated values.

TABLE II

EXPERIMENTAL RESULTS OF CUBOID

Vertex	Ground truth [m]	Estimated value [m]
p	[1.440, 1.460, 0.220]	[1.436, 1.460, 0.212]
q	[1.560, 1.460, 0.220]	[1.570, 1.457, 0.232]
r	[1.560, 1.540, 0.220]	[1.554, 1.540, 0.218]
s	[1.440, 1.540, 0.220]	[1.436, 1.539, 0.211]
t	[1.440, 1.540, 0.000]	[1.443, 1.540, 0.001]
u	[1.440, 1.460, 0.000]	[1.450, 1.461, 0.006]

TABLE III

RMSE OF CUBOID'S ESTIMATED FEATURE POINTS

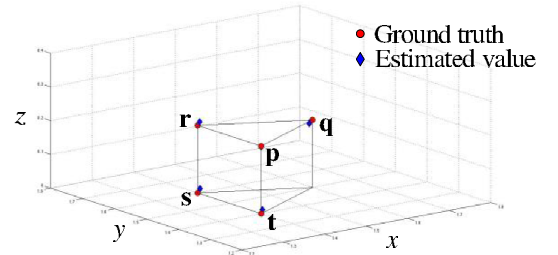| Vertex	RMSE [m]	Vertex	RMSE [m]
p	0.005	s	0.006
q	0.009	t	0.006
r	0.004	u	0.007

Fig. 7. Experimental results of triangular prism. 3-D coordinates of triangular prism's 5 vertices are estimated. The red circle marks indicate the ground truth, and the blue diamond marks indicate the estimated values.

TABLE IV

EXPERIMENTAL RESULTS OF TRIANGULAR PRISM

Vertex	Ground truth [m]	Estimated value [m]
p	[1.400, 1.400, 0.200]	[1.400, 1.400, 0.197]
q	[1.600, 1.500, 0.200]	[1.592, 1.500, 0.191]
r	[1.400, 1.600, 0.200]	[1.406, 1.601, 0.209]
s	[1.400, 1.600, 0.000]	[1.407, 1.601, 0.011]
t	[1.400, 1.400, 0.000]	[1.408, 1.407, 0.007]

TABLE V

RMSE OF TRIANGULAR PRISM'S ESTIMATED FEATURE POINTS

Vertex	RMSE [m]	Vertex	RMSE [m]
p	0.002	s	0.008
q	0.007	t	0.007
r	0.006		

VI. CONCLUSION

This paper presented the methodology to measure 3-D coordinates of feature points for 3-D reconstruction of underwater objects. Our proposed model allows to measure 3-D information of underwater objects using multiple acoustic images from different views. The approach dealt successfully with the problem on the previous research that the system cannot deal with the acoustic images from arbitrary viewpoints. Moreover, as the proposed method deals with the pixel coordinate system of acoustic image for 3-D reconstruction of underwater objects, the problem of scattering and noise in the data hardly matter the results. Study on verification for the performance of our proposed method using real acoustic images remains as future works.

ACKNOWLEDGEMENTS

(a) Beam slices of ARIS EXPLORER 3000
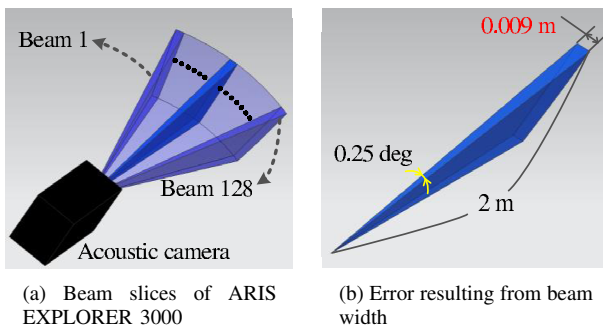
(b) Error resulting from beam width

Fig. 8. Arrange of beam slices and beam width of ARIS EXPLORER 3000. As the acoustic wave is processed by 128 array of transducers as a function of azimuth angle, error resulting from beam width is unavoidable.

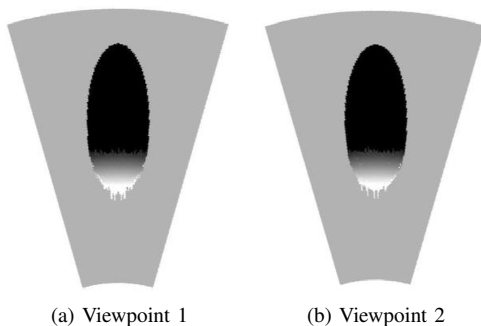(a) Viewpoint 1   (b) Viewpoint 2

Fig. 9. Acoustic images of hemisphere associated with each acoustic view. Due to absence of feature points, 3-D shape of hemisphere is identifiable. Additionally, the correspondence between two acoustic images is difficult to describe.

REFERENCES

[1] P. C. Burns, R. C. Ewing, and A. Navrotsky, "Nuclear Fuel in a Reactor Accident," *Science (Washington)*, vol. 335, no. 6073, pp. 1184-1188, 2012.

[2] R. Eustice, H. Singh, J. Leonard, M. Walter, and R. Ballard, "Visually Navigating the RMS Titanic with SLAM Information Filters," *Proceedings of the Robotics: Science and Systems*, pp. 57-64, 2005.

[3] O. Pizarro, R. Eustice, and H. Singh, "Large Area 3D Reconstructions from Underwater Surveys," *Proceedings of the 2004 MTS/IEEE OCEANS Conference and Exhibition*, vol. 2, pp. 678-687, 2004.

[4] A. Shibata, H. Fujii, A. Yamashita, and H. Asama, "Scale-reconstructable Structure from Motion Using Refraction with a Single Camera," *Proceedings of the 2015 IEEE International Conference on Robotics and Automation*, pp. 5239-5244, 2015.

[5] Y. Chang, F. Peng, L. Luo, and Y. Zhang, "Laser Imaging for the Underwater Object and the Image Segmentation Based on Fractal," *Proceeding of the 2003 International Symposium on Multispectral Image Processing and Pattern Recognition*, pp. 668-671, 2003.

[6] B. Kamgar-Parsi, L. J. Rosenblum, and E. O. Belcher, "Underwater Imaging with a Moving Acoustic Lens," *IEEE Transactions on Image Processing*, vol. 7, no. 1, pp. 91-99, 1998.

[7] V. Murino, A. Trucco, and C. S. Regazzoni, "A Probalilistic Approach to the Coupled Reconstruction and Restortion of Underwater Acoustic Images," *IEEE Transactions on Pattern Analysis and Machine Intelligence*, vol. 20, no. 1, pp. 9-22, 1998.

[8] "Blueview," 2015, retrieved June 05, 2015, from http://www.blueview.com/products/2d-imaging-sonar/p900-2250-dual-frequency.

[9] E. Belcher, W. Hanot, and J. Burch, "Dual-frequency identification sonar (DIDSON)," *Proceedings of the 2002 IEEE International Symposium on Underwater Technology*, pp. 187-192, 2002.

[10] "Aris," 2015, retrieved June 05, 2015, from http://www.soundmetrics.com/Products/ARIS-Sonars/ARIS-Explorer-3000.

[11] Y. W. Huang, Y. Sasaki, Y. Harakawa, E. F. Fukushima, and S. Hirose, "Operation of Underwater Rescue Robot Anchor Diver III during the 2011 Tohoku Earthquake and Tsunami," *Proceedings of the 2011 MTS/IEEE OCEANS*, pp. 1-6, 2011.

[12] S. C. Yu, J. H. Kim, T. Zhu, and D. J. Kang, "Development of 3D Image Sonar Based Object Recognition for Underwater Vehicle," *Proceedings of the 2012 International Offshore and Polar Engineering Conference*, pp. 502-507, 2012.

[13] S. Negahdaripour, H. Sekkati, and H. Pirsiavash, "Opti-Acoustic Stereo Imaging: On System Calibration and 3-D Target Reconstruction," *IEEE Transactions on Image Processing*, vol. 18, no. 6, pp. 1203-1214, 2009.

[14] C. Xu, A. Asada, and K. Abukawa, "A Method of Generating 3D Views of Aquatic Plants with DIDSON," *Proceedings of the 2011 IEEE Symposium on Underwater Technology and 2011 IEEE Workshop on Scientific Use of Submarine Cables and Related Technologies*, pp. 1-6, 2011.

[15] H. Assalih, Y. Petillot, and J. Bell, "Acoustic Stereo Imaging (ASI) System," *Proceedings of the 2009 IEEE OCEANS*, pp. 1-6, 2009.

[16] N. Hurtós, D. Ribas, X. Cufí, Y. Petillot, and J. Salvi, "Fourier-based Registration for Robust Forward-looking Sonar Mosaicing in Low-visibility Underwater Environments," *Journal of Field Robotics*, vol. 32, no. 1, pp. 123-151, 2015.

[17] S. Kwak, Y. Ji, A. Yamashita, and H. Asama, "Development of Acoustic Camera-Imaging Simulator Based on Novel Model," *Proceedings of the 2015 IEEE International Conference on Environment and Electrical Engineering*, pp. 1719-1724, 2015.

[18] M. D. Aykin and S. Negahdaripour, "On Feature Matching and Image Registration for Two-dimensional Forward-scan Sonar Imaging," *Journal of Field Robotics*, vol. 30, no. 4, pp. 602-623, 2013.

[19] "Specifications of ARIS EXPLORER 3000," 2015, retrieved June 05, 2015, from http://www.soundmetrics.com/Products/ARIS-Sonars/ARIS-Explorer-3000/ARIS-3000-Product-Specs-English.